Photochemical Cycle of Bacteriorhodopsin Studied by Resonance Raman Spectroscopy[†]

Manfred Stockburger,* Wilfried Klusmann, Heinz Gattermann, Günther Massig, and Reiner Peters[‡]

ABSTRACT: Individual species of the photochemical cycle of bacteriorhodopsin, a retinal–protein complex of *Halobacteria*, were studied in aqueous suspensions of the "purple membrane" at room temperature by resonance Raman (RR) spectroscopy with flow systems. Two pronounced deuterium shifts were found in the RR spectra of the all-trans complex BR-570 in H_2O–D_2O suspensions. The first is ascribed to $C{=}NH^+$ ($C{=}ND^+$) stretching vibrations of the protonated Schiff base which links retinal to opsin. The second is assigned tentatively to an "X–H" ("X–D") bending mode, where "X" is an atom which carries an exchangeable proton. A RR spectrum of the 13-*cis*-retinal complex "BR-548" could be deduced from spectra of the dark-adapted purple membrane. The RR spectrum of the M-412 intermediate was monitored in a double-beam pump–probe experiment. The main vibrational features of the intermediate M′ in the reaction

$$\text{M-412} \underset{}{\overset{h\nu}{\rightleftharpoons}} \text{M}' \xrightarrow{\Delta} \text{BR-570}$$

could be deduced from a photostationary mixture of M-412 and M′. Difference procedures were applied to obtain RR spectra of the L-550 intermediate and of two new long-lived species, R_1'-590 and R_2-550. From kinetic data it is suggested that R_1'-590 links the proton-translocating cycle to the "13-cis" cycle of BR-548. The protonation and isomeric states of the different species are discussed in light of the new spectroscopic and kinetic data. It is found that conformational changes during the photochemical cycle play an important role.

Bacteriorhodopsin, a retinal–protein complex of the purple membrane of *Halobacteria*, is capable of mediating light-to-energy conversion. The unique properties and functions of this complex were first elucidated by Oesterhelt & Stoeckenius (1973). Since then a considerable body of information has been collected by a number of authors [for a review, see Stoeckenius (1976), Henderson (1977), Oesterhelt (1976), and Lozier & Niederberger (1977)]. It is generally accepted now that retinal is attached to the protein via a Schiff base linkage. In the light-adapted purple membrane the chromophore forms a strong absorption band with a maximum around 570 nm. This "purple complex" will be denoted by "BR-570".

Following light absorption, the primary complex BR-570 runs through several intermediates with significant spectral changes and, at room temperature, is regenerated after a few milliseconds. This cyclic process is accompanied by a translocation of protons across the cell membrane. In this way an electrochemical gradient across the membrane is established which can drive ATP synthesis and transport processes. By application of flash spectroscopy, the intermediates of the cycle have been characterized by their different absorption spectra and time behavior [for a review, see Lozier & Niederberger (1977)].

In the last few years, resonance Raman (RR)[1] spectroscopy has been successfully applied to study chromophoric groups in biological systems. Rimai and his colleagues studied different retinal isomers and their Schiff bases as model compounds for the visual pigment rhodopsin (Rimai et al., 1971; Heyde et al., 1971; Gill et al., 1971). It was realized that each retinal isomer has a distinct and characteristic vibrational pattern in its Raman spectrum and that the protonation state of the Schiff base is indicated by the frequency of the C=N ($C{=}NH^+$) stretching vibration. These early results showed that the RR spectra of retinal chromophores in biological systems provide an excellent probe of the structure or of structural changes at the active site. Stimulated by this work, a number of RR studies were performed on visual pigments and related model compounds [Oseroff & Callender (1974), Mathies et al. (1976, 1977), Callender et al. (1976), and a review by Callender & Honig (1977)].

If bacteriorhodopsin and its intermediates are probed in an RR experiment by laser radiation, the photolability of these species must be taken into account. The intensity of a Raman band is expressed by a cross section for transforming an incoming photon into a scattered Raman photon. In spite of "resonance enhancement" by irradiation into the strong $\pi\pi^*$ absorption band of the chromophore, this quantity is ~6 orders of magnitude smaller than the cross section for absorbing a photon (v. Grundherr & Stockburger, 1973) and $\sim 3 \times 10^5$ times smaller than the cross section for the primary photochemical event which has a quantum yield of ~0.3 (Goldschmidt et al., 1977; Becher & Ebrey, 1977). Therefore, if a RR experiment is performed with a CW laser beam and a "fixed" sample, a photostationary equilibrium between the different species of the photocycle is established by the probe beam long before the "first" Raman photon is scattered. A photodecomposition of the sample can be avoided if a molecular flow system is used. By this method a pure RR spectrum of the BR-570 complex could be obtained by Aton et al. (1977).

In this paper we have started systematic work to obtain RR spectra of pure species and intermediates of the photochemical cycle of bacteriorhodopsin. As a starting point the time evolution of the photochemical cycle was analyzed for a typical Raman experiment in which a suspension of the purple membrane is exposed to CW laser light of constant intensity for a variable period of time. In such an experiment not only

---

[†] From Max-Planck-Institut für Biophysikalische Chemie, 3400 Göttingen-Nikolausberg, Federal Republic of Germany. *Received March 2, 1979.* The work was supported in part by the Deutsche Forschungsgemeinschaft.

[‡] Abteilung für Mikrobiologische Chemie, Klinikum der Johann Wolfgang Goethe-Universität, 6000 Frankfurt am Main, Federal Republic of Germany.

[1] Abbreviations used: RR, resonance raman; CW, continuous wave.

the primary photochemical event must be taken into account but also subsequent photochemical reactions of the intermediates induced by the incident laser radiation. The time evolution of the system is determined by two parameters, the photochemical rate constants which depend on the photon flux and the dwell time of the molecules in the laser beam.

In most of our experiments a "rotating cell" was used as a flow system in which the dwell or transit time depends on the rotation frequency. This technique, by controlling the amount of decomposition via the rotation frequency and the laser power, provides spectra of the starting material in single-beam experiments and also allows spectra of intermediates in pump–probe double-beam experiments to be recorded.

For the interpretation of intermediate spectra, we found it necessary to study again the spectra of the primary complex BR-570 in H_2O as well as in D_2O suspensions. Some important deuterium effects were detected which were not reported previously. We also found it instructive to study RR spectra of dark-adapted membrane suspension. From such spectra we were able to deduce a spectrum of the 13-cis complex "BR-548" (Oesterhelt et al., 1973).

Much interest has been focused in the past on the long-lived complex M-412 since it is the first intermediate in the pump cycle which was found to be deprotonated (Lewis et al., 1974). Evidently, the knowledge of the structure of M-412 is of much importance for the elucidation of the molecular pump mechanism. A RR spectrum of M-412 was reported by Aton et al. (1977) under conditions which appreciably lengthen the lifetime of this intermediate (4.3 M salt concentration, pH 10). We have obtained a RR spectrum of M-412 under the dynamic conditions of the pump cycle prevailing in pure aqueous suspensions at room temperature. This enabled us to obtain kinetic information about the pump cycle from photoinduced reactions of M-412 on a time scale which is short compared to the 5-ms lifetime of this intermediate.

It is well-known that M-412 undergoes a photoinduced reversion process to the primary complex BR-570 via an intermediate M′ which absorbs light in the same spectral region as M-412 (Hess & Kuschmitz, 1977; Becher & Ebrey, 1977). In a nanosecond laser experiment we were able to obtain a spectrum of a photostationary mixture of M-412 and M′ and to deduce the main vibrational features of M′ from the composite spectrum.

Of much interest are the RR spectra of the two first intermediates in the cycle, K-590 and L-550. It is impossible to prepare these species by any choice of the excitation parameters in a pure form. Therefore, one has to disentangle the composite spectra. This can be partially done by subtracting the considerable contribution of the primary complex which is always involved. In this way we were able to obtain a rather pure spectrum of L-550.

This procedure was less successful in the case of K-590. The reason is that at high irradiation, where K-590 accumulates, another so far unknown species is formed which predominates in the RR spectrum. This species finally relaxes to a long-lived intermediate (R_1'-590) from which a rather pure RR spectrum could be obtained. From the kinetic and spectroscopic behavior of R_1'-590 and from the work of Sperling et al. (1979) with respect to a conversion BR-570 → BR-548 (13-cis), it is suggested that R_1'-590 decays with a high yield to the 13-cis complex and thus forms a link between the proton-translocating and the 13-cis cycle. In a final section the protonation and isomeric states of the different intermediates will be discussed in light of our new spectroscopic results.

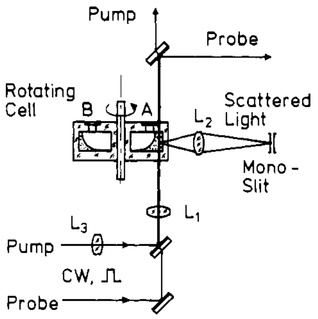

FIGURE 1: Optical design of the Raman cell illumination: L_1 (f = 100 mm), L_2 (f = 50 mm), and L_3 (f = 200 mm).

The work of Marcus & Lewis (1978) and Cookingham et al. (1978), which came to our attention after sending our manuscript for publication, was considered in the revised manuscript. The reader is also referred to the recent work of Terner et al. (1979), which is mainly concerned with the RR spectra of L-550 and BR-548. This paper came to our attention when the revised manuscript was completed.

Experimental Procedure

Optical Design. The optical design of the Raman cell illumination is illustrated in Figure 1. The sample, a highly diluted suspension of the purple membrane with an optical density of 1 at 570 nm, is enclosed in a cylindrical quartz cell, which can be rotated at variable frequency. The cell consists of two compartments, A and B, separated by a quartz plate. The optical path length of the cell is 10 mm, and the outer diameter is 45 mm with a thickness of the wall of 1.5 mm. In most experiments the sample has been irradiated by two laser beams of different wavelength: a pump beam to trigger the photochemical cycle and a probe beam to monitor the different species by Raman scattering or by optical absorption. The distance of the collinearly aligned laser beams from the cell wall is 1 mm, and the distance to the rotational axis is r_0 = 20 mm. If the lens L_3 is taken out of the pump beam, both laser beams are focused by the lens L_1 into the center of the sample. If L_3 is inserted, a parallel pump beam of 1-mm diameter traverses the cell. The Raman light which is scattered at a right angle to the probe beam is focused by the lens L_2 (f = 50 mm) with a magnification factor of 5 onto the entrance slit of a double monochromator (Spex 1302, f = 50 cm). Since the height of the entrance slit is 20 mm, a length of the probe beam of 4 mm in the middle of the sample can be fully utilized for Raman scattering.

The most important parameter for photochemical events is the photon flux in the sample. For a focused laser beam of constant power, the flux is determined by the diameter of the laser beam in the focal spot. Let us consider a CW laser beam at 514 nm with a Gaussian profile and a diameter of 2 mm, which is defined as the distance between I_0/e^2 points (I_0 is the maximum intensity). If this beam is focused by L_1 (f = 100 mm), a beam waist of Gaussian profile with a diameter d_0 of 34 μm is calculated in the focal spot. The "useful" length of the beam, where d_0 is increased by a factor of $2^{1/2}$ is 6.36 mm (Yariv, 1975). The averaged profile of the 4-mm region around the focal spot was experimentally determined by translating its fivefold magnified image across the entrance slit of the monochromator. From this profile the diameter d_0 (distance between I_0/e^2 points) was deduced. For a Gaussian profile the laser power is given by

$$P_0 = \pi(d_0/2)^2(I_0/2) \qquad (1)$$

In this paper we make the approximate assumption that the beam in the focal spot has a cylindrical intensity profile with diameter d_0 and a uniform photon flux, which according to eq 1 is given by $\bar{I} = I_0/2$. $\bar{I}$ is obtained from the laser power P_0 and the experimentally determined value of d_0. Later in this paper first-order rate constants for photochemical events will be defined which are proportional to $\bar{I}$.

Rotating Cell. A rotating cell has first been used by Kiefer & Bernstein (1971) in order to obtain Raman spectra of photolabile molecules. The virtue of this technique is that the molecules remain only for a certain transit time Δt in the beam, which can be controlled by the rotation frequency ν_0 of the cell. The transit time is given by

$$\Delta t = d_0/v \tag{2a}$$

where

$$v = 2\pi\nu_0(r_0/2) \tag{2b}$$

is the angular velocity. Thus, photolysis may be controlled by variation of the transit time Δt. In principle, this technique has the same effect as the flow methods of Mathies et al. (1976) and Callender et al. (1976). However, in the case of the light-adapted form of the purple membrane where one is concerned with a fully reversible cyclic process of a short period ($\tau = 5$ ms), the rotating cell method has the advantage that only a few milliliters of purple membrane suspension are needed for a Raman experiment. The condition $T \simeq 4\tau$ has to be fulfilled in order to make sure that the cycle is practically completed during one rotational period T of the cell. This leads to an upper limit of 50 s^{-1} for the rotation frequency, which corresponds to an angular velocity of $v = 6.28$ ms^{-1} or to $\Delta t = 6.4$ μs for a typical beam diameter of 40 μm.

Capillary Flow System. The rotating cell technique could not be used to obtain a RR spectrum of the dark-adapted purple membrane because the time constant for its reconstitution is as long as 20 min (Oesterhelt et al., 1973). For this purpose a flow system was set up whose essential part was a capillary of 1 mm diameter. The details of this experiment are described later in this paper.

Detection of the Raman Signal. The scattered and dispersed Raman light was detected by a photomultiplier (EMI, 9658, with focusing magnet) which was cooled down to −15 °C. The photocurrent was fed into a photon-counting unit which was connected with a multichannel analyzer (MCA, Canberra, Model 8100). When pulsed laser radiation was used for excitation, the Raman signal was detected by a boxcar integrator (PAR 162). The spectrometer, which is linear in wavelength, is driven with an electronically controlled stepping motor (Spex Compudrive and Repscan). This unit allows the preselection of a spectral window, the spectral width of a single step, and the number of sweeps. As a rule, a window of 28-nm width (930 cm^{-1} in the green) was divided into 1000 steps and correlated with 1000 channels of the MCA into which the number of photons during a single sweep was stored. In most cases a number of 10–20 sweeps had to be accumulated in the MCA to obtain spectra of satisfactory signal-to-noise ratios. The Raman spectra were recorded with a spectrometer slit width of 200 μm, which corresponds to 5.3 cm^{-1} (0.16 nm) in the green spectral region. The narrowest bands of the spectra had a natural width of 10 cm^{-1}, corresponding to 11 channels of the MCA. The data were transferred from the MCA to a computer. Without any further correction, the spectra were displayed as counts per channel as a function of the channel number, which is a linear function of wavelength. The scale was calibrated for each excitation line with a set of well-known Raman lines. The wavenumber shifts, obtained in this way, are accurate to ±5 cm^{-1}. Difference spectra were calculated with a computer program and displayed in the same way.

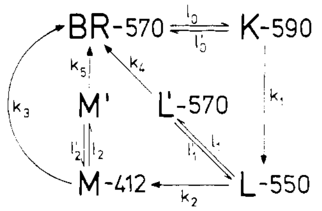

FIGURE 2: Reaction scheme from literature data. The reaction starts from the primary complex BR-570. Intermediates are assigned by capital letters and labeled by the wavelength of the absorption maxima. Photoreactions are assigned by open arrows and rate constants l_i and thermal reactions by closed arrows and rate constants k_i. At room temperature $k_1 = 5 \times 10^5$ s^{-1}, $k_2 = 2.5 \times 10^4$ s^{-1}, and $k_3 = 200$ s^{-1}. The rate constant k_3 describes the reconstitution of BR-570 from M-412. Intermediates of this reaction (N-520 and O-640) were omitted.

Absorption Measurements. Two different types of absorption measurements were carried out. In both cases the light of a tungsten filament was used to form a probe beam of small diameter and divergence. After the cell the beam was focused onto the entrance slit of a monochromator and detected at the exit slit by a photomultiplier. (1) In the first experiment the pump beam consisted of 1.6-ms pulses of rectangular wave form and a 50-s^{-1} repetition rate. These were formed from a CW laser beam at 514 nm by a mechanical chopper. The cell remained at a fixed position, and the wave form of the transmission signal, following the pump pulses, was measured at different fixed wavelengths by using the boxcar integrator technique. In this way the decay of the starting material (BR-570) and the growing-in of the long-lived intermediate (M-412) were determined as a function of the power of the pump laser. (2) In the second experiment absorption spectra of the purple membrane were recorded in the presence of CW pump radiation (514 nm) as a function of the rotation frequency. The two compartments, A and B, of the cell were filled with water and purple membrane suspension, respectively. The photocurrents I_A and I_B, which refer to the probe beam across the compartments A and B, are fed into the two channels A and B of a photon-counting device which measures $\log (I_A/I_B)$.

Light Sources. The following light sources were used: CW argon ion lasers CR2 and CR15 from Coherent Radiation, a CW tunable jet-stream dye laser Model 375 from Spectra Physics, and a nanosecond dye laser FL 1000T pumped by the N_2 laser M 2000 from Lambda Physics.

Materials. Purple membrane was isolated from *Halobacterium halobium* R_1 cells as described by Oesterhelt & Stoeckenius (1974). Samples were suspended in doubly distilled water (pH 5.6) or in heavy water of 99.75% purity. The suspensions were diluted to obtain an optical density of 1 at 570 nm.

Results and Discussion

Photochemical Effect of the Pumping Light Intensity and Duration. A kinetic scheme of the cycle is depicted in Figure 2. Photoreactions are assigned by open arrows and rate constants l_i and thermal processes by closed arrows and rate constants k_i. If the rate constants l_i are small compared with the competing k_i values, the photoinduced cross-links of the cycle can be neglected and one obtains the well-known open cycle as it emerges from low-temperature and flash-photolysis experiments [for a review, see Henderson (1977) and Lozier & Niederberger (1977)]. The open cycle is governed by the single photoreaction BR-570 → K-590 and the consecutive thermal processes with rate constants $k_1 = 5 \times 10^5\ \mathrm{s}^{-1}$ and $k_2 = 2.5 \times 10^4\ \mathrm{s}^{-1}$ at room temperature (Stoeckenius & Lozier, 1974; Dencher & Wilms, 1975). The thermal reconstitution of BR-570 from M-412 is described by an overall rate constant k_3 (200 s^{-1} at room temperature). The details of this process via different intermediates (N-520 and O-640) are not considered further in this paper.

Photoreactions of the intermediates of the cycle must be taken into account when the wavelength of the exciting laser beam lies within their optical absorption bands. The photoinduced reconstitution of BR-570 from the long-lived intermediate M-412 has been studied by several groups (Hess & Kuschmitz, 1976; Becher & Ebrey, 1977). From photostationary experiments at various low temperatures, Hurley et al. (1978) concluded that this process goes through an intermediate M′ whose absorption spectrum is only slightly different from that of M-412. A similar photoinduced process was found by these authors for the back-reaction from the intermediate L-550 to BR-570 via a transient species L′ with an absorption maximum close to 570 nm.

The rate constant for the primary photochemical event is given by

$$l_0 = \gamma_0 \sigma_0 \bar{I} \tag{3}$$

where σ_0 is the cross section for absorbing a photon from the laser beam, $\bar{I}$, as defined according to eq 1, is the photon flux of the beam (photons $\mathrm{cm}^{-2}\ \mathrm{s}^{-1}$), and γ_0 is the quantum yield of the primary photochemical event. σ is related to the molar decadic extinction coefficient by

$$\sigma = (2303/L)\epsilon$$

where L is Avogadro's number. For the laser line at 514 nm, one obtains from $\epsilon_{\max}$ (BR-570) = 63 000 $\mathrm{M}^{-1}\ \mathrm{cm}^{-1}$ (Oesterhelt & Hess, 1973) and from the shape of the absorption spectrum of BR-570 in Figure 10 a value for σ_0(514 nm) of 1.35×10^{-16} cm^2. For the quantum yield γ_0 a value of ~0.3 is reported (Goldschmidt et al., 1977; Becher & Ebrey, 1977).

The photon flux at 514 nm is given by

$$\bar{I}(514\ \mathrm{nm}) = (2.6 \times 10^{18}) P_0 / F$$

where P_0 is the laser power in watts and F is the beam area in square centimeters. If the beam is focused by the lens L_1 (see Figure 1), a diameter of $d_0 = 40\ \mu\mathrm{m}$ was determined experimentally. If these data are inserted into eq 3, one obtains

$$l_0(514\ \mathrm{nm}) = (8.4 \times 10^6) P_0\ \mathrm{s}^{-1} \tag{4}$$

for the rate constant of the primary photochemical event. A reasonable value for the maximum power of the 514-nm line for Raman experiments with purple membrane suspensions is given by $P_0 = 5$ W. From this an upper limit for l_0 of $4.2 \times 10^7\ \mathrm{s}^{-1}$ for the primary rate constant is determined.

We now consider the limiting cases of high- and low-beam intensity. The *low-intensity limit* is defined by the condition $k_1 \gg l_0 \gg k_3$ (see Figure 2). The second of these inequalities is added as we are only interested in cases where the formation of M-412 is fast compared to the slow thermal reconstitution reaction. We also make the assumption that $k_4 \gg l_1$. Under these conditions the reactions of Figure 2 may be expressed in the simple form

$$\text{BR-570} \underset{l_1}{\overset{l_0}{\rightleftharpoons}} \text{L-550} \xrightarrow{k_2} \text{M-412} \tag{5}$$

which is valid for laser irradiation above 500 nm, in which the photoreaction of M-412 can be neglected. The time dependence of the three species can be calculated analytically under the condition that light of constant intensity is switched on at $\Delta t = 0$. For a demonstration, the solution for $l_0 = l_1 = 5 \times 10^4\ \mathrm{s}^{-1}$ and $k_2 = 2.5 \times 10^4\ \mathrm{s}^{-1}$ is depicted graphically in Figure 3.

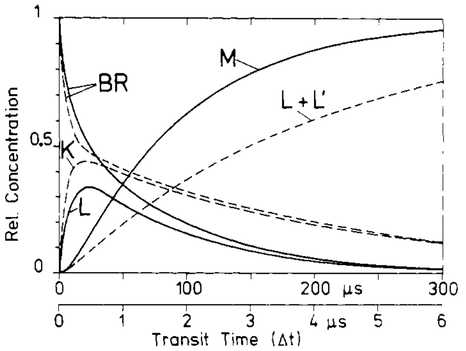

FIGURE 3: Time evolution of the primary complex BR and its intermediates K, L + L′, and M from analytical solutions of the reactions in eq 5 and 6. (—) Upper time scale, eq 5: $l_0 = l_1 = 5 \times 10^4\ \mathrm{s}^{-1}$ and $k_2 = 2.5 \times 10^4\ \mathrm{s}^{-1}$. (- - -) Lower time scale, eq 6: $l_0 = l_0' = 5 \times 10^6\ \mathrm{s}^{-1}$ and $k_1 = 5 \times 10^5\ \mathrm{s}^{-1}$.

The validity of the relation shown in eq 5 was proved as follows. The formation of M-412 was monitored as a function of the dwell time Δt in the laser beam (see Experimental Procedure, absorption measurements type 1). An "effective" rate constant k_{eff} for the formation of M-412 was measured as a function of l_0 within the low-intensity limit. k_{eff} is defined as the inverse of the time Δt_{eff} at which M-412 has reached 63% of its saturation value. The experimentally determined dependence of k_{eff} on l_0 is in good agreement with the functional relation of these two quantities derived from solutions of eq 5 under the condition $l_1 = l_0$. This result indicates that the magnitude of l_1 is indeed similar to that of l_0. Since the extinction coefficients of BR-570 and L-550 at 514 nm are close to each other (Lozier & Niederberger, 1977), it follows from eq 3 that the quantum yield for the photoinduced reconstitution from L-550 is of a similar magnitude as that for the primary photochemical event.

The *high-intensity limit* shall be defined by the condition $l_0 > k_1$ and the additional assumption that $l_1 = l_1' \gg k_4$. In this limit the kinetic situation is more complicated because the concentration of the intermediate K-590 grows up considerably, too. However, since k_2 is much smaller than k_1, the time span until saturation of M-412 is established can be divided into two time domains. In the first one, which is described by the process

$$\text{BR-570} \underset{l_0'}{\overset{l_0}{\rightleftharpoons}} \text{K-590} \xrightarrow{k_1} \text{L} + \text{L}' \tag{6}$$

the starting material finally is completely converted into the two intermediates L and L′. The time dependence of this reaction for the special conditions $l_0 = l_0' = 5 \times 10^6\ \mathrm{s}^{-1}$ and $k_1 = 5 \times 10^5\ \mathrm{s}^{-1}$ is depicted in Figure 3. In the second time domain, which is determined by the rate constant k_2, the conversion of L + L′ to M-412 is accomplished.

The transit time Δt of a material flow across the laser beam is determined by the beam diameter d_0 [defined according to eq 1] and the frequency ν_0 of the rotating cell (see eq 2a,b). Both parameters were varied in our experiments. We shall consider the two limiting cases where the laser beam is focused to $d_0 = 40\ \mu\mathrm{m}$ (case 1) or is adjusted to a width of 1 mm (case 2). In the first case, the fivefold magnified image of the beam waist just fills the width of the monochromator slit of 200 μm (see Figure 1). For a fixed transit time Δt_0 the contribution of a certain species to the RR spectrum is given by its concentration averaged over Δt_0. This is equivalent to an integration of the time-dependent concentration functions from

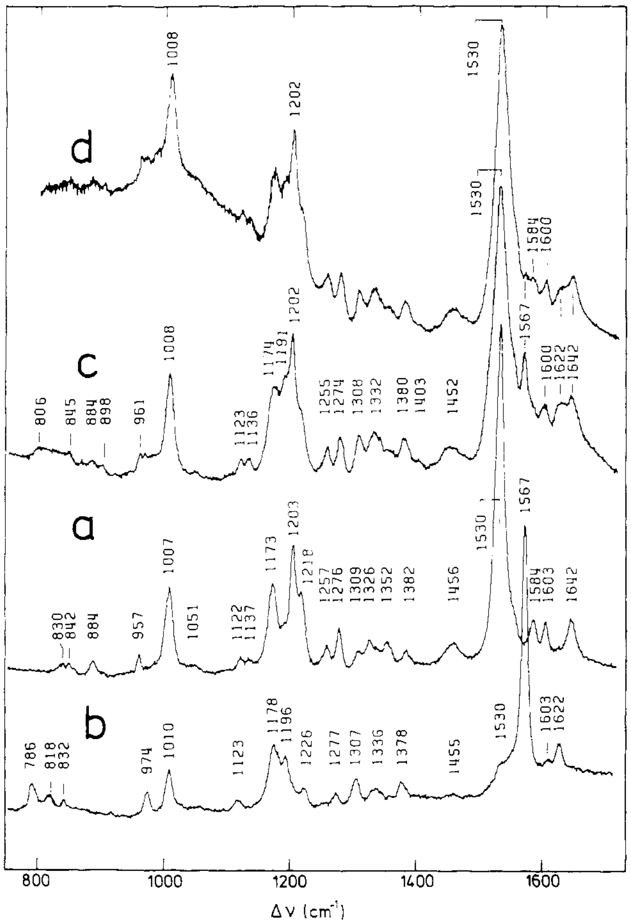

FIGURE 4: Resonance Raman spectra of different species of the photochemical cycle. (a) BR-570: 514-nm excitation and $l_0\Delta t_0$ = 0.1. (b) Long-lived intermediate M-412, obtained in a double-beam experiment: pump radiation 514 nm, probe radiation 457 nm, and $l_2\Delta t \ll 1$. (c) Mixture of long-lived intermediates R_i and M-412: 514-nm excitation, $l_0 = 2 \times 10^6$ s^{-1}, and Δt = 0.3 ms. The band at 1567 cm^{-1} is due to the intermediate M-412. (d) Same conditions as in (c), however, with additional pump radiation at 457 nm ($l_2\Delta t \gg 1$) which causes a decrease of the 1567-cm^{-1} band (M-412) by a factor of 5 and an increase of the RR intensity of all other bands by a factor of 2.5. These factors are not considered in the intensity scale of the spectra (c) and (d).

Δt = 0 to Δt_0. In the second case, where d_0 is 1 mm, the monochromator slit is small compared to the fivefold magnified image of the beam waist. The slit is set into the middle of this image. Under such conditions the Raman signal probes the concentration of a certain species at a transit time $\Delta t = d_0/2v$. This configuration was preferentially used in double-beam experiments where the pump beam is large, whereas the probe beam is focused and aligned in the middle of the pump beam.

In the following sections various Raman experiments will be described in which single laser beams or combinations of pump and probe beams were used to monitor RR spectra of the different species in the photochemical cycle. The analysis of this section makes evident that for each of these experiments the rate constants l_i and the transit time Δt must be known for a critical evaluation of the results.

Of special interest is the RR spectrum of the primary complex excited by a focused laser beam (cf. case 1 above). For $l_0\Delta t_0 \ll 1$, this decays according to $\exp(-l_0\Delta t)$ and $l_0\Delta t_0$ gives the relative decrease during Δt_0. In our experiments $l_0\Delta t_0$ = 0.1 was used, which assures that 95% of the primary complex contributes to the RR spectrum.

RR Spectrum of BR-570 in H_2O Suspension. The RR spectrum which was obtained with the rotating cell ($l_0\Delta t_0$ = 0.1, 514 nm) is depicted in Figure 4a. Our spectrum is very similar to that reported by Aton et al. (1977), which was obtained with a capillary flow method and 568-nm excitation. Only minor differences in the intensity of the bands between 1580 and 1650 cm^{-1} exist, which are due to the different excitation wavelength.

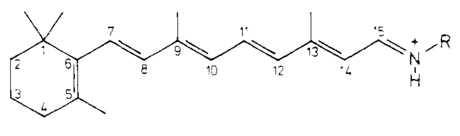

FIGURE 5: *all-trans*-Retinal, bound to a residue R via a protonated Schiff base linkage.

A flow spectrum of BR-570 was recently reported by Markus & Lewis (1978). In their spectrum a band at 1185 cm^{-1} and a shoulder at ~1550 cm^{-1} appear which are not seen in the spectrum of Figure 4a. According to our experience, these two features are only observed when the condition $l_0\Delta t \ll 1$ is not fulfilled and intermediates already contribute to the spectrum.

The spectrum of BR-570 will serve as a reference for all other spectra which will be presented throughout this paper. Therefore a brief analysis is given which is based on comparison with model compounds. From biochemical evidence it is concluded that the BR-570 complex consists of retinal in the all-trans form which is bound to the ε-amino group of a lysine residue via a Schiff base linkage (see Figure 5). As model compounds, the spectra of *all-trans*-retinal and its Schiff bases have been studied by several groups (Heyde et al., 1971; Callender et al., 1976; Mathies et al., 1977; Aton et al., 1977; Cookingham et al., 1978).

Due to the influence of the two different terminal groups and the substitution in the C(9) and C(13) positions, the various double and single bonds of the isoprenoid chain of retinal are not exactly equal in strength. Therefore, this unit has to be considered rather as a "single molecule" than as a chain with repetitive units. This implies that a manifold of vibrational modes of different frequency exists which would be degenerated in an extended chain. For instance, in polyenes only the stretching modes are Raman active (Inagaki et al., 1975). Thus, one obtains for a polyene with seven double bonds two strong RR bands (ν_1 = 1535 cm^{-1}; ν_2 = 1146 cm^{-1}) of comparable intensity (v. Grundherr & Stockburger, 1973; Margulies & Stockburger, 1979).

The strongest bands in the RR spectra of retinal will be those which involve C=C, C—C, and C—CH_3 stretching motions in their normal coordinates because these give rise to large Franck–Condon factors. The strongest feature in the RR spectra of isoprenoid chains is expected for the C=C stretching mode. In the spectrum of BR-570 a single band (14-cm^{-1} half-width) is observed at 1530 cm^{-1} for this vibration. This means that the four double bonds of the chain have nearly identical frequencies. There is also no clear evidence for an extra band which could be assigned to the double bond in the cyclohexene ring. Two other weak features (1584 and 1603 cm^{-1}) have frequencies close to those of isolated double bonds. It is very unlikely, however, that such bonds exist in BR-570. There is also no clear evidence for these two bands in the spectra of model compounds. Thus, it seems that they are typical features of the BR-570 complex.

It was found empirically that ν(C=C) depends linearly on λ_{max} of the optical absorption band in a way that a red shift of λ_{max} is accompanied by a downfield shift in ν(C=C) (Heyde et al., 1971). Both effects are due to a delocalization of the π electrons which may be caused by protonation of the Schiff base or in biological systems by a variety of influences (Honig et al., 1976). It should be noted that the shift of $\nu(C{=}C)$ is a ground-state effect while the excited state plays a dominant role for the shift of λ_{max}. The $\nu(C{=}C)/\lambda_{max}$ correlation will be used later in this paper.

On the basis of spectroscopic studies on retinal analogues by Cookingham et al. (1978), some characteristic bands in the "fingerprint" region (1100–1400 cm^{-1}) can be assigned. In the spectrum of BR-570 the normal coordinates of the most distinguished bands at 1203 and 1173 cm^{-1} can be described as C—C stretch/C—CH_3 rock and C—C stretch vibrations, respectively. A weaker band at 1276 cm^{-1} is attributed to a C—C—H bend/C—C(C=C) stretch coordinate. The region between 900 and 1100 cm^{-1} is dominated by the band at 1007 cm^{-1} which is composed of C—CH_3 stretching vibrations, mainly at the C(9) and the C(13) positions (Cookingham & Lewis, 1978). The weak band at 957 cm^{-1} has been assigned as a C—H out-of-plane bending vibration (Rimai et al., 1971).

Of great importance are the Raman bands which arise from the Schiff base group. It has been concluded from model compounds that a weak band near 1620 cm^{-1} is mainly due to the isolated C=N stretching of the unprotonated Schiff base linkage. In the protonated form of the Schiff base, a band of medium intensity near 1655 cm^{-1} arises which was assigned to the stretching vibration of the $C{=}NH^+$ group (Heyde et al., 1971; Aton et al., 1977). It will be shown that this characteristic vibration occurs at 1642 cm^{-1} in the RR spectrum of BR-570.

It was the main idea behind the Raman studies of model compounds in solution to identify the isomeric state of the retinal moiety in a biological chromophore. This is based on the fact already mentioned that each retinal isomer has a distinct and characteristic vibrational pattern in the fingerprint region of its Raman spectrum. Thus, one would expect that the RR spectrum of BR-570 and the spectra of the all-trans protonated Schiff base (PSB) models (Mathies et al., 1977; Aton et al., 1977; Cookingham et al., 1978) are fairly identical. This, however, is not the case. A number of less intense bands are observed in the spectrum of BR-570 which do not appear in the all-trans PSB spectra.

Two reasons could be responsible for this discrepancy. The first is that the intensity of RR bands of the isoprenoid chain depends critically on Franck–Condon factors and therefore also on slight conformational distortions induced by the protein environment. The second is that normal vibrations of environmental groups, especially in the vicinity of the protonated Schiff base, may be coupled to the π-electron system of retinal and therefore become Raman active. The two bands at 1584 and 1603 cm^{-1} are candidates for this type of interaction.

Spectra of model compounds may serve as a first guide but do not allow unequivocal conclusions with respect to the isomeric structure of the chromophore. For instance, the spectrum of BR-570 exhibits resemblance with both the 13-cis and the all-trans PSB isomer.

As was pointed out by Marcus & Lewis (1978), this dilemma can only be overcome by simulating the protein chromophore by suitable model compounds. Another approach is in principle possible by computational simulation of RR spectra of chromophoric groups. The first attempts in this direction were made by Warshel & Karplus (1974) and by Warshel & Dauber (1977).

Deuterium Effect in the RR Spectrum of BR-570. It could be shown by Oseroff & Callender (1974) that in a D_2O suspension of the visual pigment rhodopsin the frequency of a band assigned as the $C{=}NH^+$ stretch of the Schiff base linkage moves from 1655 cm^{-1} in H_2O to 1630 cm^{-1} in D_2O. It was argued that a shift of this magnitude is to be expected if one assumes that the reduced mass of an isolated oscillator $HC{=}NH^+$ is increased by replacing the proton by a deuteron. Therefore, this experiment was considered to be a proof that the Schiff base in rhodopsin is protonated.

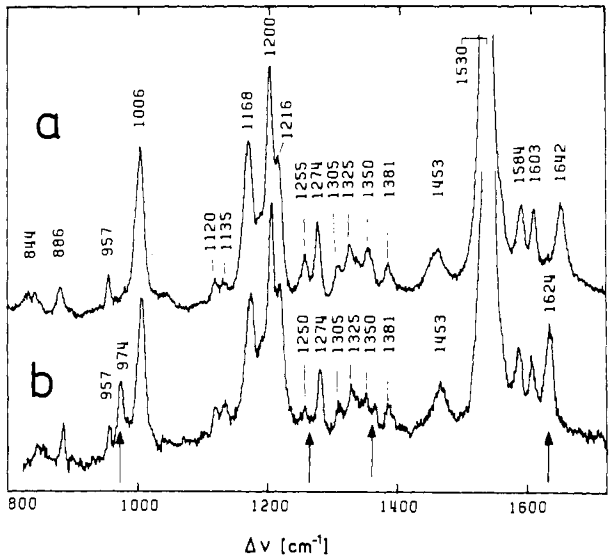

FIGURE 6: RR spectra of BR-570 in (a) H_2O and (b) D_2O suspensions of the purple membrane. Excitation in both cases was at 514 nm and $I_0\Delta t_0 = 0.1$. Deuterium effects are indicated by arrows.

It was the aim of our own experiments to detect deuterium effects which can be ascribed to the primary complex BR-570. The RR spectrum of a purple membrane suspension in D_2O was recorded under the condition $I_0\Delta t_0 = 0.1$ and compared with the spectrum in H_2O. As can be seen in the spectra of Figure 6, deuterium effects occur at four different positions.

The most remarkable effect in the spectra of Figure 6 is the shift of a band from 1642 cm^{-1} in H_2O to 1624 cm^{-1} in D_2O. Using the arguments of Oseroff & Callender (1974), we conclude that this band is essentially a $C{=}NH^+$ stretch, which implies that a protonated Schiff base also exists in the BR-570 complex of bacteriorhodopsin.

The second remarkable effect is the appearance of a new band at 974 cm^{-1} in the D_2O spectrum, and the third effect is the intensity decrease of the 1255-cm^{-1} band on deuteration. Though the intensity of the new band is nearly 2 times greater than the intensity loss at 1255 cm^{-1}, it is tempting to assign these two bands to the same vibrational mode. The only one which could account for such a large deuterium shift would be an "X–H" ("X–D") in-plane bending vibration. As is suggested from other molecules (Dewar & Ford, 1977), its frequency may well be in the 1100-cm^{-1} region. If one takes a hydrogen atom, which carries out torsional motions about a fixed atom "X", as the most simple model, one would expect a frequency decrease by a factor of $2^{1/2}$ on deuteration. The factor observed is only 9% smaller. The intensity gain on deuteration could in principle be explained by an increase of the Franck–Condon factors. This is conceivable for such a large frequency change since the potential surfaces remain fairly unchanged by replacing the proton by deuterium.

If one accepts that the Schiff base nitrogen is the only atom in the BR-570 complex which is able to carry an exchangeable proton, X would be identical with this nitrogen atom. In the final section of this paper the identity of X will be discussed in more detail.

A different interpretation of the new band at 974 cm^{-1} was given by Marcus & Lewis (1978). They assume that the band at 957 cm^{-1} in H_2O is composed of several accidentally de-

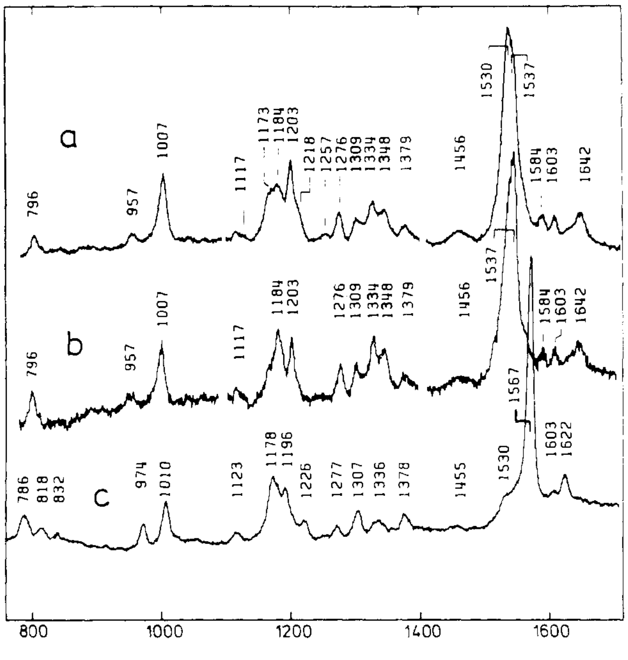

FIGURE 7: (a) RR spectrum of a dark-adapted purple membrane suspension, excited at 514 nm. (b) Spectrum of BR-548 (13-cis) obtained by a difference procedure (see text). (c) Spectrum of M-412 as in Figure 4b.

generate C–H bending vibrations. One of the components then is supposed to increase in frequency on deuteration of the Schiff base nitrogen. This assumption would require that the 957-cm^{-1} band loses much of its intensity in the D_2O spectrum. This, however, is clearly not the case (cf. Figure 6), which makes this interpretation very unlikely.

The fourth deuterium effect is observed close to 1350 cm^{-1}, where a small dip in the D_2O spectrum corresponds to a clearly developed band in the H_2O spectrum. This effect, like the previous ones, is also detected in a H_2O/D_2O difference spectrum.

RR Spectrum of the Dark-Adapted Purple Membrane. So far we were concerned with the light-adapted purple membrane. In the dark an equilibrium is established (in 20 min at 35 °C) between the all-trans complex (BR-570) and a 13-cis complex (BR-548) to which both components contribute with equal amounts (Oesterhelt et al., 1973; Sperling et al., 1977).

The RR spectrum of the dark-adapted purple membrane was recorded with a capillary flow system. A suspension of 700 mL of purple membrane (OD = 1) was kept in a dark vessel and then pumped through a capillary tube of 1-mm diameter at a velocity of 3 ms^{-1} to a second dark vessel. Excitation was carried out with a focused laser beam (d_0 = 40 μm) of 8 mW at 514 nm. With the assumption that the extinction coefficients of the two components have the same magnitude at 514 nm, the rate constant of light adaption

$$\text{BR-548} \xrightarrow[I_{\text{DL}}]{h\nu} \text{BR-570}$$

has a value of 8×10^3 s^{-1}, which follows from eq 3 and 4 by taking a quantum yield of 3.5×10^{-2} for this process (Kalisky et al., 1977). Then for the product $I_{\text{DL}}\Delta t_0$ (Δt_0 = 13.3 μs), a value of 0.1 is obtained which assures that the spectrum in Figure 7a involves BR-548 to at least 95% of its natural abundance in the dark. For recording the spectrum in Figure 7a, we pumped the 700-mL suspension 60 times across the capillary. Care was taken that the sample was in the dark-adapted form before a single run was started.

In order to obtain a spectrum of the 13-cis complex, we had to subtract the contribution of BR-570 and its intermediates to the composite spectrum. For this purpose a spectrum of the light-adapted purple membrane suspension was recorded under the same conditions as were applied for the dark-adapted form. The subtraction procedure was based on the observation that in the composite spectrum the intensity of the band at 1257 cm^{-1} is by more than a factor of 2 lower than in the spectrum of BR-570 (cf. Figures 4a and 7a, taking the C–CH_3 stretch at 1007 cm^{-1} as an internal intensity standard) and therefore only represents the 50% contribution of BR-570. As a second condition, it was assumed that from the two overlapping C=C bands in the spectrum in Figure 7a only the high-frequency component at 1537 cm^{-1} prevails in the spectrum of BR-548. The spectrum, obtained in this way, is depicted in Figure 7b.

Intermediates M-412 and M′. The longest lived intermediate in the photocycle is M-412, which at room temperature reconverts slowly (k_3 = 200 s^{-1}) to the primary complex. Figure 3 illustrates the formation of M-412 at a pump rate of 5×10^4 s^{-1}. For this rate, which according to eq 4 corresponds to a laser power of only a few milliwatts, the saturation of M is already obtained in the millisecond time domain.

A RR spectrum of M-412 was recorded in a pump–probe beam experiment. A parallel pump beam (514 nm, d_0 = 1000 μm) was obtained by inserting the lens L_3 confocal to L_1 (cf. Figure 1). The probe beam at 457 nm was focused to d_0 = 50 μm and was aligned so as to pass through the center of the broad pump beam. The parameter $I_0\Delta t$ of the pump beam was adjusted in a way to reach the saturation concentration of M-412 in the center of the beam. For the 457-nm probe radiation the condition $I_2\Delta t \ll 1$ had to be taken into account in order to avoid photoconversion of the M-412 complex.

The spectrum obtained is demonstrated in Figure 4b. With the exception of the weak wing at 1530 cm^{-1}, it represents the pure M-412 intermediate. The spectrum of M-412 differs in essential ways from that of BR-570 (cf. parts a and b of Figure 4). The blue shift in $\lambda_{\max}$ (absorption) from 570 to 412 nm is correlated with an upfield shift of ν(C=C) from 1530 to 1567 cm^{-1}. Direct evidence for the protonation state of this species is obtained from the Raman spectrum in that we could not find any deuterium effect. On the basis of model compound spectra, the band at 1622 cm^{-1} is assigned to the C=N vibration of a nonprotonated Schiff base linkage.

The vibrational pattern in the fingerprint region, in particular between 1170 and 1230 cm^{-1}, is also very different from that of BR-570. The band at 1257 cm^{-1} which was tentatively assigned by us to an X–H bending vibration is not observed in the M-412 spectrum. This would be expected for an unprotonated species. Another difference is the shift of the 957-cm^{-1} band of BR-570 to 974 cm^{-1} in the case of M-412. Of much interest is also the relatively strong band group around 800 cm^{-1} which has no counterpart in the spectrum of BR-570.

A spectrum of M-412, obtained under similar conditions, was recently reported by Marcus & Lewis (1978). With respect to the main bands, their spectrum is identical with ours, although a few weak features appear to be different. In particular, the characteristic band group around 800 cm^{-1} is not reported by these authors.

To obtain a spectrum of M′, a photostationary mixture of M-412 and M′ (cf. Figure 2) was established. M-412 was prepared by CW radiation in the same way as described in this section. A second parallel beam was focused (40 μm) in

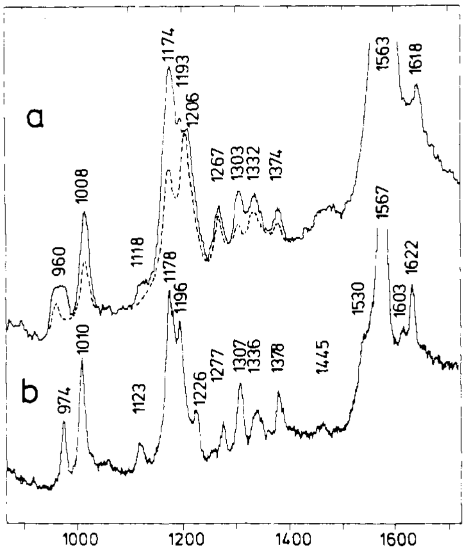

FIGURE 8: (a) RR spectrum from a photostationary mixture of the intermediates M-412 and M′ established by 514-nm CW and 435-nm pulsed (nanosecond) radiation. The spectrum was probed by the 435-nm beam. The dotted spectrum refers to M′ (see text). (b) RR spectrum of M-412 as in Figure 4b.

the center of the 514-nm beam. It consisted of 453-nm dye laser pulses of 50-μJ energy and 6-ns duration, giving $I_2 = 7 \times 10^9\ s^{-1}$ and $I_2\Delta t = 36$. Under such conditions the photostationary equilibrium between the two components is established within a time interval which is short compared to 6 ns. Therefore, the equilibrium composition of the two components is probed by the 435-nm radiation. The RR spectrum of the mixture is depicted in Figure 8a. It is different from the spectrum of pure M-412 in Figure 8b.

From the two spectra in Figure 8 it is possible to deduce the spectrum of M′ if the relative contribution of the two components to the equilibrium spectrum is known. We made the assumption that M-412 and M′ contribute with a relative concentration of 1:1 to the equilibrium spectrum. This is justified by the fact that the absorption spectra of the two components are nearly identical (Hurley et al., 1978). The relative Raman intensity of M-412 and M′ was established on the basis of the assumption that the C–CH_3 stretch (1008 cm^{-1} in the composite spectrum) has the same Raman intensity for both components. In order to obtain the spectrum of M′, we had to subtract about half of the intensity of the spectrum of M-412 in Figure 8b then from the composite spectrum in Figure 8a.

The difference in bandwidth of the two spectra in Figure 8 did not allow an exact computation of a difference spectrum. However, if one takes the peak height as a measure of intensity, such a spectrum can be approximately obtained (see dotted line from 900 to 1400 cm^{-1} in Figure 8a). It is significantly different from the spectrum of M-412. In particular, the intensity ratios of the strongest bands at 1178/1196 and 1174/1206 cm^{-1}, respectively, are reversed when going from M-412 to M′. A similar change is observed for the band pairs at 1277/1307 and 1267/1303 cm^{-1}, respectively. The spectral changes suggest that the photochemical process $\text{M-412} \xrightarrow{h\nu} \text{M}'$ constitutes an isomerization of retinal. Since M′ thermally relaxes rapidly to the original complex BR-570 (Hurley et al., 1978), it is very likely that the chromophores in M′ and BR-570 have a similar geometry. It is interesting, therefore, to compare the spectra of the two species in the fingerprint region, taking into account that the band at 1257 cm^{-1} is characteristic of the protonated complex and is therefore not expected to appear in the spectrum of M′. With the exception of the band at 1350 cm^{-1}, the residual bands of the two species exhibit a remarkable similarity in the fingerprint region with respect to frequency as well as to intensity distribution. If one considers the spectra of deprotonated Schiff bases (Aton et al., 1977; Marcus & Lewis, 1978), the closest relationship is found between the spectrum of M′ and the all-trans model compound. From this analysis much support is given to the assumption that M′ like BR-570 entails retinal in the all-trans configuration.

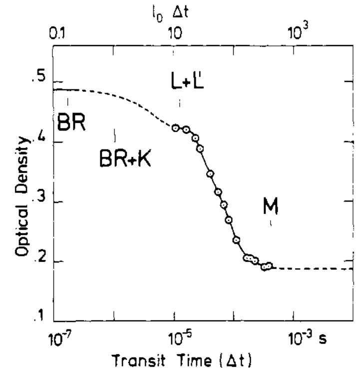

FIGURE 9: Optical density of an aqueous suspension of the purple membrane, monitored by a CW laser beam (514 nm), as a function of the transit time Δt across the laser beam. The measured values (⊙) correspond to $I_0 = 10^6\ s^{-1}$. The limiting values on both ends of the scale were obtained by varying both I_0 and Δt. The time domains of the different species BR, K, L, L′, and M are indicated.

Which conclusions can be drawn from RR spectra with respect to the structure of the intermediate M-412? By comparing the spectrum of M-412 with the spectra of deprotonated Schiff bases of retinal, Marcus & Lewis (1978) came to the result that the isomeric state of the chromophore in M-412 is essentially all-trans. This was based on the fact that five bands between 1150 and 1230 cm^{-1} in the spectra of M-412 and the all-trans model compound coincide in frequency. One can object against this procedure in that only a limited part of the spectrum is considered. Taking account of the complete structure in the fingerprint region, we rather came to the conclusion that there is more resemblance between the spectra of M-412 and the 13-cis model compound. However, we again point out that unequivocal conclusions cannot be drawn from model compound spectra.

It is very likely that the photochemical process $\text{M-412} \xrightarrow{h\nu} \text{M}'$ constitutes an isomerization of retinal. From our own results, which point to an all-trans configuration of retinal in M′, it is therefore suggested that M-412 entails retinal in an isomeric state which is different from the all-trans form.

Long-Lived Intermediates in the Prestationary State. The time domain in which M-412 approaches its upper concentration limit (cf. Figure 3) shall be denoted by the term prestationary state.[2] RR spectra recorded under such conditions probe long-lived species like M-412 but not those intermediates which precede M-412 in the cycle. In this section it will be demonstrated by absorption and RR experiments that in addition to M other long-lived intermediates

---

[2] The notation "stationary" is reserved to situations with light of constant intensity and a sample in a fixed position in which also the slow reconstitution reaction of BR-570 from M-412 is considered ($k_3 = 200\ s^{-1}$). No significant change in the Raman spectra was observed when going from the prestationary to the stationary case because k_3 in all experiments was small compared to I_0. We preferred experiments in the prestationary state which correspond to rotation frequencies of 0.5–5 s^{-1} for the cell. Under such conditions thermal effects which play a role at high laser power can be avoided.

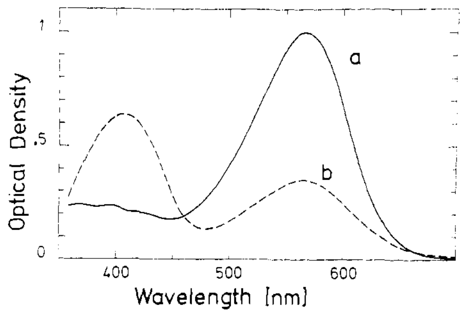

FIGURE 10: Absorption spectra of the purple membrane in aqueous suspension. The spectra are corrected for the background which is caused by scattered light. (a) Spectrum of BR-570; and (b) spectrum obtained with an additional pump beam whose parameters I_0 and Δt correspond to the lower OD limit in Figure 9.

exist which absorb light in the region between 500 and 600 nm.

In Figure 9 the optical density (OD) of a purple membrane suspension, which is exposed to laser radiation at 514 nm, is depicted as a function of $I_0\Delta t$. In this experiment the laser beam both photolyzes and probes the sample. Let us first consider the time domain 10^{-5} s $< \Delta t < 10^{-3}$ s, keeping I_0 at 10^6 s^{-1}. Around 10^{-5} s the OD values form a plateau (OD = 0.42). With increasing Δt the optical density decreases and at ~0.3 ms reaches a final value of 0.19. This does not decrease further, even in the limiting case $I_0\Delta t \rightarrow \infty$, which was achieved by keeping the sample in a fixed position. The other limit, $I_0\Delta t \rightarrow 0$, was approached by decreasing I_0 to $\sim 10^4$ s^{-1} and leaving Δt at 10^{-5} s. An OD value of 0.49 is then obtained, which obviously corresponds to the primary complex BR-570. The plateau around 10^{-5} s is in the time domain of L-550. Its conversion to M-412 is reflected by the subsequent decrease to the residual OD value of 0.19 in the prestationary state.

The spectral distribution of the residual absorption is shown in Figure 10. For comparison, the spectrum of BR-570 is also depicted. The maximum of the residual absorption lies close to 570 nm, where it amounts to 35% of the absorbance of BR-570. Its spectral distribution, however, is different from BR-570 in that the relative absorbance with respect to BR-570 increases on both sides of the maximum. This behavior suggests that various compounds "R_i" (residual) contribute to this spectrum. When the bleaching experiment of Figure 9 was performed with 568-nm radiation, a residual absorption of 28% was found at this wavelength in the prestationary state.

The Raman intensity, represented by the peak height of the $C-CH_3$ stretch at 1007 cm^{-1}, decreases in a similar way as the optical density when going from $\Delta t = 10^{-5}$ s to the prestationary state. A Raman spectrum which was recorded under prestationary conditions is depicted in Figure 4c ($I_0 = 2 \times 10^6$ s^{-1}, $\Delta t = 3$ ms, 514 nm). It can be expected that this spectrum involves all the compounds R_i which contribute to the residual absorption. The RR spectrum in Figure 4c differs in many details from that of BR-570. Thus, new bands occur at 1191 and 1622 cm^{-1} and in the region between 1300 and 1400 cm^{-1}. On the other hand, many common features also exist. The band at 1567 cm^{-1} in the spectrum in Figure 4c obviously is due to the C=C stretch of M-412. This is confirmed by the fact that it completely vanishes for 568-nm excitation under prestationary conditions (cf. Figure 11i). The occurrence of this band in the spectrum in Figure 4c allows an experiment which further elucidates the long-lived species R_i.

In this experiment two CW laser beams (514 and 457 nm) were aligned collinearly and focused into the cell. The 514-nm beam has two functions. First, it acts as a pump beam to establish prestationary conditions. Second, it probes intermediates by their RR scattering and optical absorption. When the power of the 457-nm beam was raised, the C=C stretch of M-412 decreased in intensity while all other bands in the spectrum in Figure 4c increased. This effect could be saturated by increasing the power to $I_2 > 5 \times 10^5$ s^{-1}. A spectrum which is recorded under such conditions is shown in Figure 4d. With the exception of the C=C band of M-412, the vibrational structure in this spectrum is identical with that of Figure 4c. (The background on the low-frequency side of the spectrum

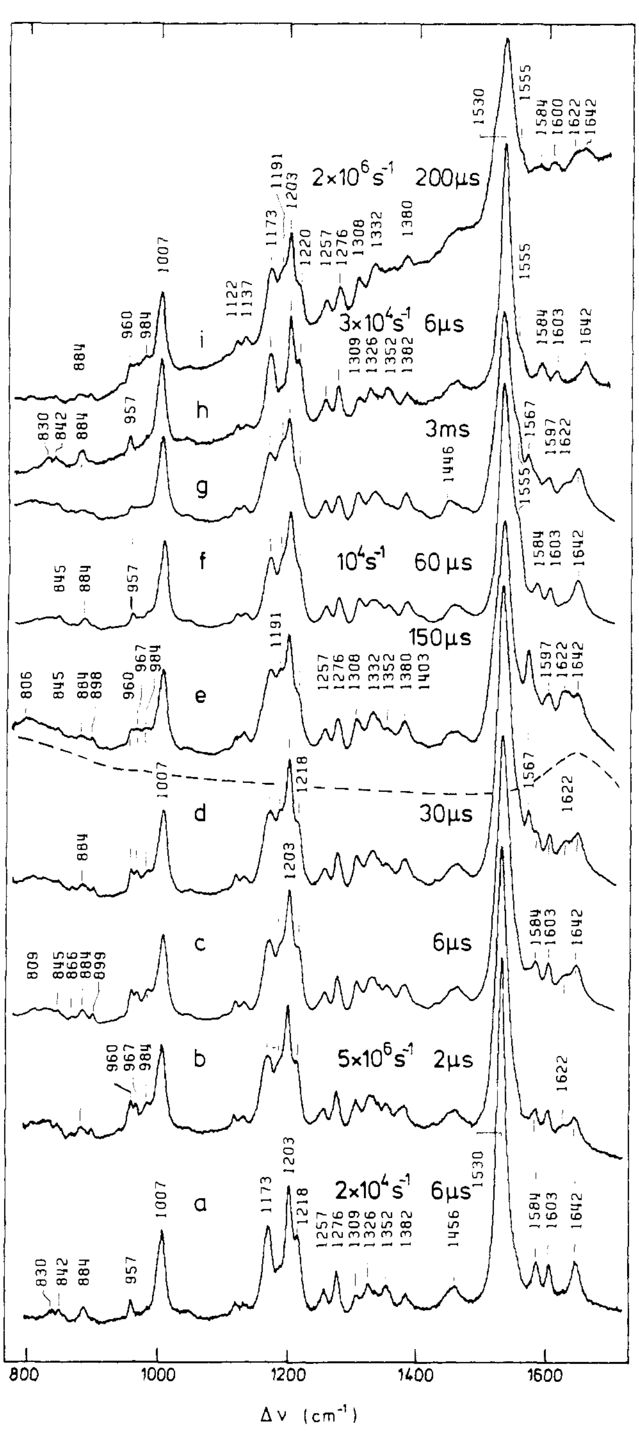

FIGURE 11: RR spectra of the purple membrane of various values of I_0 and Δt. (a) BR-570 as in Figure 4a; (b–e) 514-nm excitation, $I_0 = 5 \times 10^6$ s^{-1}, and Δt = 2, 6, 30, and 150 μs; (f, g) 514-nm excitation, $I_0 = 10^4$ s^{-1}, and Δt = 60 μs and 3 ms; and (h, i) 568-nm excitation. (h) $I_0 = 3 \times 10^4$ s^{-1} and Δt = 6 μs; this is essentially the spectrum of BR-570; (i) $I_0 = 2 \times 10^6$ s^{-1} and Δt = 200 μs.

is caused by the broad O–H stretching vibration of water which is excited by the 457-nm beam.) This implies that the composition of the species R_i which is probed by the 514-nm line does not depend on the presence of the 457-nm radiation. Under saturation conditions of the 457-nm radiation, it was found that the intensity of the C═C band of M-412 is lowered by a factor of 5, while the intensity of all other vibrational features which represent the species R_i is increased by a factor of 2.5. The second part of this result was confirmed by the observation that the optical density, monitored at 514 nm, also is increased by a factor of ~2.5. From these experiments we can conclude that in the saturation limit the concentration of M-412 is lowered by a factor of 5, while that of the species R_i is increased by a factor of 2.5.

In the prestationary state the species M-412 and R_i obviously are the only ones which accumulate. Let us make the assumption that the species R_i are represented by a mean extinction coefficient which is equal to that of BR-570 at 570 nm. Then one obtains from the absorption spectra of Figure 10 for the molar fraction of the two types of species

$$[\mathrm{R}_i] + [\mathrm{M\text{-}412}] = 0.35 + 0.65 = 1$$

When the 457-nm radiation is raised to the saturation limit, one obtains on the basis of the RR spectroscopic results

$$[\mathrm{R}_i] + [\mathrm{M\text{-}412}] = 0.875 + 0.13 \approx 1$$

The fact that M-412 is not completely converted into R_i could be due to an incomplete overlap of the two laser beams.

The result of this section can be summarized in a simplified manner by the reaction scheme

$$\mathrm{M\text{-}412} \underset{l_2'}{\overset{l_0'}{\leftrightarrows}} \mathrm{BR\text{-}570} \underset{(l_r')}{\overset{l_i'}{\rightleftarrows}} \mathrm{R}_i \tag{7}$$

The rate constants l are proportional to the light intensity (cf. eq 3) only for low-intensity values. At high intensity the rates are often limited by thermal relaxation processes, i.e., l_0' by k_2 and l_2' by k_5 (cf. Figure 2). It is possible that l_i' is also limited by such a process.

It is important to note that a strong light-induced back-reaction from R_i to BR-570 is not consistent with the experimental results. Consider the case where the sample is irradiated by 568-nm laser light and therefore l_2' can be completely neglected. If a strong back-reaction would occur ($l_r' \approx l_i'$), all material should be in the M-412 complex when the prestationary state is reached. What is observed, however, is a residual absorption of 28% at 568 nm whose RR spectrum is given in Figure 11i. This implies that $l_r' \ll l_i'$. The spectrum in Figure 11i is identical with the spectra in parts c and d of Figure 4 with the exception of the C═C stretch of M-412.

In the spectra of the species R_i, many vibrational features of the primary complex BR-570 are preserved (cf. parts a and c of Figure 4 and parts h and i of Figure 11). In all cases a peak is observed at 1530 cm^{-1} which is consistent with the fact that the residual absorption has its maximum close to 570 nm. From this observation it is tempting to conclude that BR-570 is involved in the spectra of the species R_i. A concentration of BR-570 of 10–20% in the prestationary state, as is estimated from the spectra, would require that both $l_2' \approx 0.4 l_0'$ and $l_r' \approx 0.4 l_i'$. This, however, is inconsistent with the experimental results. The spectroscopic behavior could be understood if a component within the long-lived species R_i would exist which has a similar structure and therefore also a similar spectrum to BR-570. On the other hand, the reaction scheme of eq 7 may be too simple to account for reactions which allow for a residual amount of BR-570 in the prestationary state (cf. Extended Reaction Scheme section below). At the moment, we are unable to decide between these two possibilities. In any case, there exists a RR spectrum in the prestationary state which is closely related to the spectrum of BR-570.

In this context, it is interesting to mention an experiment of Becher & Ebrey (1977). They found that, under conditions where the lifetime of M-412 is appreciably increased (low temperature, high salt concentration, pH 10), the purple complex is completely bleached. Under such conditions the species R_i are obviously completely converted into M-412.

Formation and Spectra of the Intermediates R_i, L-550, and K-590. An interesting feature in the spectra of the species R_i is the band at 1622 cm^{-1} (cf. Figure 4c). This band coincides in frequency with the C═N stretch of a deprotonated Schiff base (cf. with the spectrum of M-412 in Figure 4b). The time dependence of the 1622-cm^{-1} band has previously been studied by Marcus & Lewis (1977) and by Campion et al. (1977). They found that this band already occurs for Δt values of a few microseconds and concluded that deprotonation during the photocycle might already occur in an intermediate which precedes M-412.

In our own time-resolved experiments, we considered the evolution of complete RR spectra as a function of l_0 and Δt. Some typical spectra are shown in Figure 11. All spectra were normalized with respect to the intensity of the $\mathrm{C{-}CH_3}$ stretch at 1007 cm^{-1}. It is assumed that the RR cross section of this band is nearly invariable for the different species and therefore can be used as an internal intensity standard. For a rough estimation of RR intensities, we assume that the total RR cross section of the 1007-cm^{-1} band, which is the sum of the contributions of individual species in a single spectrum, has a constant value for excitation at the same wavelength. This is based on the fact that all components except M-412 absorb in the spectral region from 500 to 600 nm and at similar strength. In this way, it is possible to estimate the relative contribution of single species from the intensity of characteristic bands in the spectra of Figure 11.

Let us consider the spectra in Figure 11b–e which were obtained for $l_0 = 5 \times 10^6\ \mathrm{s}^{-1}$ and various values of Δt by excitation at 514 nm. At $\Delta t = 2\ \mu\mathrm{s}$ the 1622-cm^{-1} band can be already well identified. Even a spectrum obtained at $\Delta t = 1\ \mu\mathrm{s}$ and $l_0 = 5 \times 10^6\ \mathrm{s}^{-1}$ is nearly identical with the 2-μs spectrum and exhibits this band as a clearly resolved feature. In the microsecond domain the two bands at 967 and 984 cm^{-1} appear together with the 1622-cm^{-1} band. We therefore attribute these three bands to the same species which is now denoted by the special term "R_1". In the time domain from 6 μs to the prestationary state which is established at 150 μs, the relative intensity of the 1622-cm^{-1} band increases by nearly a factor of 2. For estimating the change of the absolute intensity, it has to be taken into account that the RR intensity, represented by the standard band at 1007 cm^{-1}, decreases by a factor of ~3 when going from 2 μs to 150 μs and keeping all other parameters constant. This implies that the absolute intensity of the 1622-cm^{-1} band varies only slightly from 2 to 150 μs. On the other hand, it is suggested from a change of the intensity of the 1622-cm^{-1} band with respect to the two bands at 967 and 984 cm^{-1} (cf. Figure 11b–e) that the species R_1 changes during this period. It is therefore assumed that R_1 relaxes to a slightly different species R_1' in the prestationary state (cf. Figure 13).

So far we have considered spectra of the species R_i in the high-intensity limit. A spectrum which was obtained in the low-intensity limit under prestationary conditions is shown in Figure 11g ($l_0 = 10^4\ \mathrm{s}^{-1}$). This differs in some details from the spectrum in Figure 11e. In particular, the 1622-cm^{-1} band is lower in intensity by a factor of ~3 while at 1555 cm^{-1} a shoulder appears as a new feature. Also the C=C stretch of M-412 appears to be weaker. On the other hand, the two spectra are very similar in the fingerprint region.

As long as the prestationary state is not established the spectra of Figure 11 contain a certain amount of BR-570. Following the discussion of the previous section, it is assumed that also in the prestationary state a species is partially involved whose spectrum is essentially identical with that of BR-570. In this section the attempt will be made to subtract the spectrum of BR-570 from the composite spectra in Figure 11.

We start this procedure with the spectrum in Figure 11f which was obtained in the low-intensity limit (I_0 = 10^4 s^{-1}) at Δt = 60 μs. According to analytical solutions of eq 5 taking $I_0 = I_0'$ = 10^4 s^{-1} and k_2 = 2.5 × 10^4 s^{-1}, one obtains for the relative concentrations of the three components BR, L, and M at Δt = 60 μs (unfocused laser beam) values of 62, 18, and 20%, respectively (compare Figure 3 for solutions with $I_0 = I_0'$ = 5 × 10^4 s^{-1}). In order to obtain the contribution of the three components to the RR spectrum, we have to multiply these numbers by factors which are proportional to the RR cross sections at 514 nm. In the present case of unresolved absorption bands, the RR cross sections are approximately proportional to the optical extinction coefficients. If this is considered, one finally obtains contributions of 73, 26, and 1% for BR, L, and M, respectively [for extinction coefficients, see Lozier & Niederberger (1977) and Becher et al. (1978)].

In order to subtract the contribution of BR from the spectrum in Figure 11f, one has to look for spectroscopic labels which indicate BR-570 in an unequivocal manner. A candidate is the band at 1584 cm^{-1}. In fact its intensity in the spectrum in Figure 11f is significantly lower than in the spectrum of BR-570 (Figure 11a), a behavior which is expected from the computational arguments of this section. It was argued previously in this paper that the 1584-cm^{-1} band cannot be assigned to the retinal moiety of BR-570 but nevertheless is a band which characterizes this complex and could not be identified in the spectrum of M-412 (cf. Figure 4b).

It is conceivable that the 1584-cm^{-1} band is due to a vibrational mode of a group which is closely attached to the retinal chromophore and may become RR active by electronic coupling with the π system of the retinal chain. If this group is spatially removed from retinal, the 1584-cm^{-1} band would vanish.

A second characteristic band of BR-570 lies at 884 cm^{-1}. This band is also not observed in the spectrum of M-412. It will be used as a label for BR in those cases where the 1584-cm^{-1} band is obscured by the C=C stretch of M-412 at 1567 cm^{-1}.

When a fraction of 58% of the spectrum of BR (Figure 11a) was subtracted from the spectrum in Figure 11f, the band at 1584 cm^{-1} disappeared. The difference spectrum obtained in this way is shown in Figure 12f. This spectrum then essentially reflects the intermediate L. The weak band at 1622 cm^{-1} indicates that the species R$_1$ contributes to this spectrum only to a small amount. If this is neglected for the moment, it turns out from the spectroscopic difference procedure that the spectrum in Figure 11f consists of 58% BR and 42% L, while contributions of 73% and 27% were estimated on the basis of eq 5. The agreement is satisfactory if one takes into account that approximations were used in both procedures.

The strongest band in the spectrum of L at 1537 cm^{-1} (Figure 12f) obviously corresponds to the C=C stretch of this species. From the ν(C=C)/λ_{max} correlation, one obtains λ_{max} = 548 nm for L, in good agreement with the flash spectroscopic results [the following coordinates (cm^{-1}/nm) were used for the ν(C=C)/λ_{max} correlation: BR-570, 1530/568; BR-548, 1537/548; M-412, 1567/412; and BR-603 ("blue membrane", unpublished experiments), 1510/603].

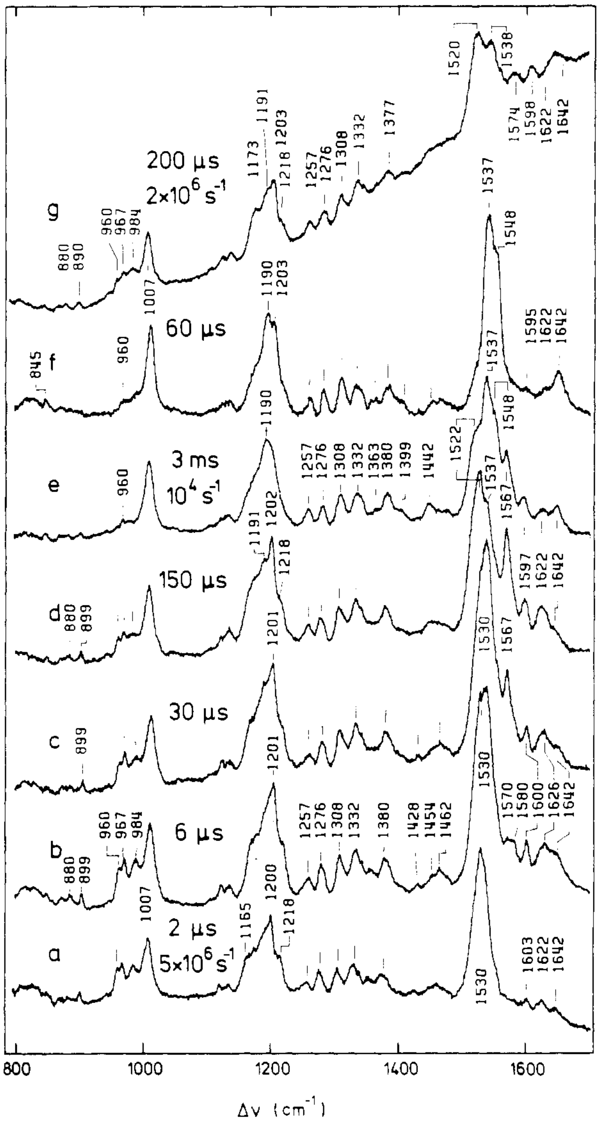

FIGURE 12: Difference spectra. Each spectrum is obtained by subtracting a certain percentage of the spectrum of BR-570 in Figure 11a from one of the spectra in Figure 11. (a) 11b – 54% 11a; (b) 11c – 46% 11a; (c) 11d – 52% 11a; (d) 11e – 37% 11a; (e) 11g – 40% 11a; (f) 11f – 58% 11a; and (g) 11i – 50% 11h. Details of the difference procedure are described in the text. The spectra (d)–(f) mainly reflect the intermediates R$_1'$-590, R$_2$-550, and L-550.

We will now discuss the difference spectra in parts d and e of Figure 12 which correspond to the prestationary state in the high- and low-intensity limits, respectively (the two spectra were obtained by subtracting 37 and 40% of the spectrum in Figure 11a from the spectra in parts e and f of Figure 11, respectively). Obviously, these spectra consist of two different components which are characterized by C=C stretching vibrations at 1522 and 1537 cm^{-1}, respectively. In the high-intensity limit (Figure 12d) the band at 1522 cm^{-1} is the strongest one, while in the low-intensity limit the 1537-cm^{-1} peak dominates. Evidently, the C=C stretch at 1522 cm^{-1} is correlated with the 1622-cm^{-1} band and consequently with the species R$_1'$. Since 1522 cm^{-1} corresponds to λ_{max} = 590 nm, this species is designated by R$_1'$-590. The band at 1537 cm^{-1} which dominates in the low-intensity limit represents a species which absorbs at λ_{max} = 550 nm and therefore is designated by R_2-550.

The existence of two species R_1' and R_2 is also nicely demonstrated by the spectrum in Figure 12g (568-nm excitation) which was obtained by subtracting 50% of the spectrum in Figure 11h from that in Figure 11i. The subtraction procedure could be based in this case on both labels (884 and 1584 cm^{-1}) since the spectra are not perturbed by the C=C stretch of M-412 at 1567 cm^{-1}. Two peaks at 1520 and 1538 cm^{-1} are obtained. Since the spectrum refers to the high-intensity limit, the 1520-cm^{-1} peak is the stronger one.

The formation of the species R_2-550 can be explained by a comparison of the two spectra in parts e and f of Figure 12. The spectrum in Figure 12e can be considered as being obtained from the spectrum in Figure 12f by increasing Δt from 60 μs to 3 ms and keeping I_0 constant. During this transition the RR intensity of the standard band at 1007 cm^{-1} decreases by a factor of 3 which is mainly due to a conversion of L to M-412. On the other hand, as was demonstrated above, the concentration of R_1 (R_1') does not change significantly during this period. This is the reason why the contribution of the species R_1 (R_1'), manifested by the two bands at 1522 and 1622 cm^{-1}, is significantly greater in the spectrum in Figure 12e than in 12f. Besides these changes, there are many features in the spectrum of L (Figure 12f) which are preserved in the spectrum of the prestationary state (Figure 12e). This is the case for the C=C stretch at 1537 cm^{-1} and the shoulder at 1548 cm^{-1} as well as for the bands in the fingerprint region, particularly for the characteristic triplet at 1363, 1380, and 1399 cm^{-1}, respectively. From this behavior we conclude that the intermediate R_2-550 is a relaxation product of the intermediate L-550.

An interesting feature in the difference spectrum in Figure 12f is the band at 1548 cm^{-1} which was designated in the original spectra in parts f and g of Figure 11 as a shoulder at 1555 cm^{-1}. This shoulder exhibits its maximum intensity under conditions where one expects the maximum concentration of L. On the other hand, it can be concluded from the spectra in parts e and f of Figure 12 that the 1548-cm^{-1} band decays in the same way as the C=C stretch at 1537 cm^{-1}. From this behavior it is suggested that the 1548-cm^{-1} band is either a feature of L or of a species which is strongly coupled to L and therefore reacts in a similar way as the intermediate L does. In this context it is interesting to note that the shoulder at 1555 cm^{-1} was attributed by Marcus & Lewis (1978) to the C=C stretch of a new species "X". From their data they concluded that X is a deprotonated species and follows on L in the photochemical cycle. We agree with these authors that such a species could play a role in the cycle, but further kinetic and spectroscopic data are necessary for a final judgement.

We will now consider the formation of the primary intermediate K, which at room temperature only can accumulate in the high-intensity limit. Under the condition $\Delta t \ll (k_2^{-1},k_4^{-1})$, the time evolution of the components BR, K, and L + L′ is given by the reaction scheme in eq 6. Analytical solutions for $I_0 = I_0' = 5 \times 10^6$ s^{-1} are presented graphically in Figure 3. From these one obtains the relative concentrations by which the components BR, K, and L + L′ contribute to the RR spectra by integration from $\Delta t = 0$ to Δt_0 (focused laser beam). For Δt = 2 μs, values of 44, 37, and 19% are obtained for the three components, respectively. The relative RR intensities are obtained by multiplying these values by factors which are proportional to the extinction coefficients at 514 nm. Using the data of Lozier & Niederberger (1977), one obtains contributions of 48, 26, and 25% for BR, K, and L + L′, respectively. According to our hypothesis that the 1584-cm^{-1} band is a label for BR, one expects from these numbers that the intensity of this band decreases by a factor of ~2 when going from the spectrum of BR (Figure 11a) to the spectrum in Figure 11b. An inspection of the two spectra reveals that this is indeed the case. From the difference procedure based on the 1584-cm^{-1} band, one obtains a contribution of 54% BR in the spectrum in Figure 11b.

The contribution of the species R_1 to the spectrum in Figure 11b, which is manifested by the band at 1622 cm^{-1}, is estimated in the following way. As was pointed out, the concentration of R_1 (R_1') changes only slightly in the time domain from 2 μs to the prestationary state where a residual absorption of 35% was found at 570 nm. This corresponds to a relative concentration of ~35% of the sum of the components R_1 (R_1'), R_2, and BR. From the spectrum in Figure 12d, we conclude that in the high-intensity limit about half of the residual species are in the R_1 complex. This implies that R_1 approximately contributes 18% to the spectrum in Figure 11b. Since the contribution of BR is 54%, it follows from the preceding discussion that the residual components in the spectrum in Figure 11b consist of 14% K and 14% L + L′. Thus, if the contribution of BR is subtracted from the spectrum in Figure 11b, the difference spectrum in Figure 12a would consist of 39% R_1, 30% K, and 30% L + L′.

It is tempting to assign the new features in the spectrum in Figure 12a, the 1622-cm^{-1} band and the three bands at 960, 967, and 984 cm^{-1}, to the intermediate K and not to a new species R_1. If this were so, the components L and L′ would dominate in the spectrum in Figure 12b at Δt = 6 μs (cf. Figure 3). This would imply that the 1622-cm^{-1} band and the bands in the 970-cm^{-1} region were the most characteristic features of L. This, however, is in disagreement with the spectrum of L which we obtained in the low-intensity limit. In this spectrum these features only play a minor role (cf. Figure 12f).

In the C=C stretching region of the spectrum in Figure 12a, a relatively broad band with a half-width of 30 cm^{-1} (14 cm^{-1} for BR) occurs which peaks at 1530 cm^{-1}. This band involves the C=C stretching vibrations of K-590 and L-550 which are expected at 1518 and 1537 cm^{-1}, respectively. The intensity distribution of this band, which is fairly symmetric with respect to 1530 cm^{-1}, suggests that the C=C stretch of R_1 is close to 1530 cm^{-1} (R_1-570). The band at 1642 cm^{-1} in the spectrum in Figure 12a is assigned to the components K and (L + L′). In the spectrum in Figure 12b, two weak features grow in at 1570 and 1580 cm^{-1} which are probably due to L′ since they are not observed in the spectrum of L (cf. Figure 12f). The most significant change in the C=C and the 970-cm^{-1} region is observed when the prestationary state is established at 150 μs. As was shown above, in this state the species R_1'-590 can be identified as the dominating one. The series of spectra in Figure 12a–d give clear evidence that the intensity ratio of the 1622-cm^{-1} band to the band group at 970 cm^{-1} increases as a function of Δt, which confirms our assumption that in the high-intensity limit two intermediates, R_1-570 and R_1'-590, occur. From Figures 12a–d, a relaxation time for the transition from R_1 to R_1' on the order of 50 μs was estimated.

Some remarks still have to be made which concern the "difference procedure" applied to the spectra in Figure 11. Although this procedure was based on spectroscopic criteria, there remains some room for free choice for the operator. This is due to the limited accuracy by which the two weak bands at 1584 and 884 cm^{-1} can be brought to zero intensity. This

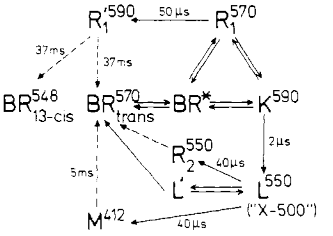

FIGURE 13: Reaction scheme of the prestationary state. Photoreactions are assigned by open arrows and radiationless transitions and thermal reactions by closed arrows. The dotted lines refer to the slow thermal relaxation processes of the long-lived intermediates. The values given for thermal decay times refer to room temperature.

is lowest for the two spectra in the prestationary state (parts d and e of Figure 12) where the 1584-cm^{-1} band is obscured. In these two cases BR was subtracted to such an extent that the weaker of the two bands in the C=C region (1522 and 1537 cm^{-1}) just appeared as a shoulder. In all cases, however, the characteristic features of the spectra remained unchanged when the subtracted amount of BR was within a "reasonable" limit.

In the prestationary state the concentration of material which absorbs light between 500 and 600 nm is lower by about a factor of 3 compared with the initial concentration of BR-570 (cf. Figure 10). The RR scattering of the residual material has decreased by a similar factor, which means that the contribution of the water band at 1640 cm^{-1} becomes significant. This is demonstrated by the dotted line in Figure 11e. In the spectra which refer to the prestationary state the intensity distribution in the region between 1500 and 1700 cm^{-1} therefore is influenced by this band. However, artificial features cannot be formed because the water band is too broad and flat. In spite of this, we have subtracted the contribution of water from the spectra in parts d and e of Figure 12.

Extended Reaction Scheme. The reaction scheme in Figure 13 represents the formation and decay of long-lived intermediates. The early appearance of the 1622-cm^{-1} band ($\Delta t = 1\ \mu$s) suggests that the species R_1 either is formed directly via an excited transition state (BR*) or is a product of K-590. From spectroscopic data it could be concluded that the formation of R_1 increases as a function of light intensity. The species R_1'-590 is a relaxation product of R_1 and therefore exhibits the same dependence on the light intensity as R_1. From RR spectroscopic evidence it is suggested that R_2 is a relaxation product of L-550.

In the prestationary state and for values of I_0 between 10^4 and 5×10^6 s^{-1}, the two species R_1' and R_2 are always observed simultaneously. In the high-intensity limit, however, the formation of R_1' dominates. A comparison of the 1622-cm^{-1} band in the spectra of parts e and g of Figure 11 reveals that the concentration of R_1' with respect to R_2 increases by about a factor of 3 when the laser power ($\sim I_0$) is raised by a factor of 500. This implies that the light-induced reaction which favors R_1 and R_1' is a nonlinear and slowly varying function of I_0. The main reason for this behavior must be seen in the fact that the products R_1, K, and L absorb the excitation light at 514 or 568 nm with a similar strength as the primary complex BR-570. Thus, in the high-intensity limit photoinduced back-reactions of the products to BR-570 may occur, as is well-known for K and BR. Processes of this type, as they are indicated in Figure 13, then may result in a rather complicated dependence of the products R_1 and R_1' on the light intensity.

Of great interest in this context is a recent experiment of Sperling et al. (1979), who determined the isomeric composition (trans and 13-cis) of a sample of bacteriorhodopsin after it had been exposed to flash light of 2-ms duration at varying intensities.[3] The samples were probed when the intermediates had relaxed after the flash either to the trans (BR-570) or to the 13-cis (BR-548) isomer. We are interested in the experiment which was started with a light-adapted sample (100% BR-570). By use of our own terminology, the results can be described as follows. Below a threshold of $I_0 = 3 \times 10^3$ s^{-1} for the light intensity no 13-cis isomer was detected. Above the threshold an increasing amount of 13-cis isomer was found which reached a limit of 20% for the highest intensity of $I_0 = 3 \times 10^5$ s^{-1}. From this behavior the authors concluded that a photoinduced conversion from the trans to the 13-cis cycle exists [for the two cycles, see Dencher et al. (1976) and Sperling et al. (1977)].

The experimental conditions during the flash ($\Delta t = 2$ ms and $I_0 = 3 \times 10^3$–3×10^5 s^{-1}) are similar to those in the prestationary state. This suggests looking for a correlation between the intermediates in this state and the final isomeric products. Thus, the threshold conditions for the formation of the 13-cis isomer are close to the conditions which were defined by us as the low-intensity limit ($I_0 = 10^4$ s^{-1} and $\Delta t = 3$ ms). In this limit the concentration of R_1', represented by the shoulder at 1522 cm^{-1} in the spectrum in Figure 12e, is small. If I_0 is raised, the 1522-cm^{-1} band increases continuously and is strongest in the high-intensity limit ($I_0 = 5 \times 10^6$ s^{-1}) of the spectrum in Figure 12d. It was estimated that under such conditions 18% of the starting material is in the intermediate R_1'. Obviously, the concentration of R_1' in the prestationary state depends in a similar way on I_0 as the amount of the 13-cis isomer which is detected after the flash. From this behavior it is suggested that the 13-cis isomer is formed from BR-570 via the intermediate R_1'-590, as is indicated in Figure 13.

It is well-known from the analysis of the 13-cis cycle (Dencher et al., 1976) that a long-lived intermediate (designated by ^{610}C) exists which decays in 37 ms preferentially to BR-548. We propose mainly from kinetic arguments that this intermediate is identical with the long-lived species R_1'-590. An additional argument for this proposal is based on absorption maxima. The label "610" denotes the maximum of the difference spectrum (^{610}C − BR-548) (Dencher et al., 1976). The maximum of the absorption peak of ^{610}C, however, must be shifted somewhat to the green and could be close to 590 nm, which is the absorption maximum of R_1'-590.

From the existence of a threshold it was concluded by Sperling et al. (1979) that the 13-cis isomer is formed from K-590 in a photoreaction. This process is implicitly involved in the reaction scheme of Figure 13. The formation of BR-548 via R_1 and R_1' may also be influenced in the high-intensity limit by the light-induced feedback reaction from L-550 and the consecutive decay of BR* to R_1. It must be emphasized that the reaction scheme of Figure 13 is by no means complete. Thus, a photoconversion of ^{610}C (R_1'-590) to BR-548 as well as photoinduced transitions from the 13-cis to the trans cycle has been reported (Dencher et al., 1976; Sperling et al., 1979). This means that in the high-intensity limit the 13-cis cycle is very likely also involved in the formation of the prestationary state. No indication for the presence of BR-548 was found in the spectra of the prestationary state in the high-intensity limit. This means that the photoinduced reactions from the 13-cis to the trans cycle are faster than those in the opposite direction.

---

[3] We are grateful to Dr. W. Stoeckenius, who brought our attention to a relationship between the work of Sperling et al. (1979) and part of our own results.

Final Discussion. It was one main goal of this paper to obtain spectroscopic evidence for the protonation and isomeric states of the different species of the photochemical cycle. Both qualities shall be finally discussed in light of our new spectroscopic data.

It could be confirmed that the protonated and deprotonated Schiff base linkages of the retinal chromophore are manifested in the RR spectra by the two bands at 1642 and 1622 cm^{-1}, respectively. In this paper we found a band at 1257 cm^{-1} which is also sensitive to the protonation state of the chromophore (cf. Figure 6). The behavior of the two proton-sensitive labels is demonstrated by a comparison of the RR spectra of L-550 and M-412 (cf. Figures 12f and 4b). The presence of the 1642-cm^{-1} band in the spectrum of L-550 indicates that in this species the Schiff base linkage is protonated. From this and the fact that the 1257-cm^{-1} band has the same relative intensity in the spectra of L and BR, it is suggested that the protonation state of L-550 is the same as that of BR-570.

A dramatic change, however, is observed in the spectrum of M-412, where the 1642-cm^{-1} band is shifted to 1622 cm^{-1} and the 1257 cm^{-1} band vanishes. The lack of any effect in the spectrum of M-412 in D_2O suspension proves that this species is completely deprotonated. Previously, in this paper we had assigned the 1257-cm^{-1} band to a X–H in-plane bending vibration. If one accepts the conventional assumption that only the proton at the Schiff base nitrogen is exchanged during the transition from L to M, X would be identical with this nitrogen atom. Some doubts with respect to this identity already arise from a comparison with protonated Schiff base model compound spectra reported by Marcus & Lewis (1978) in which no vibration in the vicinity of 1257 cm^{-1} is observed which changes in D_2O suspension. Additional arguments with respect to the identity of X are inferred from the new intermediate R_1'-590.

Consider the spectrum of R_1'-590 in Figure 12d which is characterized by a strong band at 1622 cm^{-1}. From the conventional interpretation of this band it follows that in this species the Schiff base is deprotonated. Indeed, the 1622-cm^{-1} band does not change its position in D_2O suspension. On the other hand, the relative intensity of the 1257-cm^{-1} band has the same magnitude as in the spectrum of BR-570. From this it follows that during the formation of R_1' from BR-570 the X–H group remains unchanged while the Schiff base is deprotonated. The spectroscopic behavior thus suggests that in the chromophore two different sites exist to which exchangeable protons are attached.

It is interesting to note that the deprotonated Schiff base of R_1'-590 is not correlated, as would be expected, with a blue shift of the absorption peak. On the contrary, a small red shift to 590 nm is observed. An explanation for this behavior could be that instead of a proton a hydrogen atom is abstracted from the Schiff base and the positive charge stays within the chromophore.

In this context, it is interesting to note that the spectrum of BR-548 (13-cis) in Figure 7b exhibits the $C{=}NH^+$ stretch at 1642 cm^{-1} but no band at 1257 cm^{-1}. This does not mean that no vibration of the X–H bending type exists. It is rather supposed that this band is shifted in frequency. This might also be explained by the fact that two different sites in the chromophore are responsible for the two vibrations.

If one accepts that the two spectroscopic labels indicate two protons at different sites in the chromophore, it would follow that during the transition from L-550 to M-412 two protons are transferred from the chromophore to a proton acceptor. It is conceivable that this process consists of two consecutive steps via the intermediate "X-500" which had been attributed by Marcus & Lewis (1978) to a deprotonated species which occurs before M-412. However, it should be kept in mind that all statements with respect to two different protons sites are based on our tentative assignment of the 1257-cm^{-1} band to a X–H bending vibration. This may be confirmed or rejected by future work.

A model was suggested by Schulten & Tavan (1978) in which proton translocation is supposed to be coupled to the motion of the Schiff base nitrogen which is induced by conformational changes of the isoprenoid chain. The model is essentially based on the fact that energy barriers for isomerization strongly depend on the protonation state of the different species of the cycle (Orlandi & Schulten, 1979). It was argued that the primary photochemical event consists of simultaneous rotation about the 14–15 single and 13–14 double bond. This would imply that the intermediate L-550 would be in a 13-cis, 14-cis conformation while the intermediate M-412 would be essentially in the 13-cis configuration since in the deprotonated state there is nearly free rotation about the 14–15 single bond.

How do the spectroscopic results fit into this model? As was argued in this section, L-550 has the same protonation state as BR-570. The differences in the RR spectra therefore can be ascribed exclusively to structural changes during the transition from BR-570 to L-550 (cf. Figures 4a and 12f). The most significant changes in the spectra occur in the 1150–1250-cm^{-1} region. In the spectrum of BR-570 three strong bands appear in this region at 1173, 1203, and 1218 cm^{-1}, respectively. In the spectrum of L-550 a new strong band is growing in at 1190 cm^{-1} while the two bands at 1173 and 1218 cm^{-1} are only observed as faint shoulders. The significant weakening of the 1173-cm^{-1} band, which was assigned to a C–C stretch of the isoprenoid chain, indicates that the length of the unperturbed chain is shortened by conformational changes. It is supposed that the new band at 1190 cm^{-1} is characteristic of a cis configuration. It is remarkable that the intensity of the 1203-cm^{-1} band remains nearly unchanged. This can be explained by the nature of its normal mode (C–C stretch/C–CH_3 rock) which is mainly concentrated at the C(9) and C(13) positions and therefore is less dependent on conformational changes. Significant changes are also observed in the 1300–1400-cm^{-1} region where the band at 1308 cm^{-1} is increased in the spectrum of L-550 while the typical BR-570 band at 1352 cm^{-1} vanishes.

In the spectrum of M-412 the most significant changes with respect to L-550 are caused by the change in the protonation state (cf. Figures 4b and 12f). However, some similarities are also observed in the two spectra. Thus, in the 1300–1400-cm^{-1} region the three characteristic bands of L at 1308, 1332, and 1380 cm^{-1} are also found in the spectrum of M-412. It is very likely that the bands in the region between 1150 and 1250 cm^{-1} change in frequency when going from L to M. Thus, the band pair at 1203/1190 cm^{-1} of L could correspond to the pair at 1196/1178 cm^{-1} of M. The similarities of the two spectra imply that the isomeric states of the two species are very similar to each other.

In this context, it is interesting to consider the RR spectrum of the dark-adapted complex BR-548 which, according to biochemical evidence, entails retinal in the 13-cis configuration. Obviously, BR-548 and M-412 cannot be in the same isomeric state since their kinetic behavior is quite different. It was conjectured by Schulten (1978) that dark adaption is accomplished by simultaneous rotation about the 13–14 and 15–16 double bonds which results in a 13-cis, 15-cis configuration of BR-548. A comparison of the spectra of BR-548 and L-550 (Figures 7b and 12f) reveals a similar structure in the 1150–1250-cm^{-1} region, although the cis peak of BR-548 is shifted down from 1190 to 1184 cm^{-1}. When the spectra of BR-548 and M-412 are compared (cf. parts b and c of Figure 7), one again has to consider the difference in the protonation state which may account for frequency shifts of corresponding bands in the 1150–1250-cm^{-1} region. It is quite remarkable that only these two species exhibit fairly strong bands in the 800-cm^{-1} region.

Finally, we consider the spectrum of R_1'-590 (Figure 12d). If our proposal is accepted that this species is identical with the long-lived intermediate ^{610}C in the 13-cis cycle, it would follow from a conjecture of Schulten (1978) that R_1'-590 is in the 15-cis configuration. The spectrum of R_1' indeed exhibits remarkable differences with respect to BR-548. Typical for R_1' is the intensity distribution of the three bands at 1308, 1332, and 1380 cm^{-1} and the absence of any feature at 1352 cm^{-1}. On the other hand, there exist also minor differences with respect to L-550 in the 1150–1250-cm^{-1} region as well as in the 1300–1400-cm^{-1} region.

Although we are unable at the moment to identify precisely isomeric states from RR spectroscopic features, it can be concluded from the significant spectral changes in the 1150–1400-cm^{-1} region that conformational changes play an important role in the photochemical cycle. The fact that such changes are already observed for the intermediate L-550 supports the assumption of Schulten & Tavan (1978) that the primary event constitutes a photoisomerization. So far biochemical evidence exists only for the all-trans and 13-cis forms of retinal in bacteriorhodopsin and its intermediates (Oesterhelt et al., 1973; Dencher et al., 1976; Pettei et al., 1977). It is very likely therefore that L-550 and M-412 are in the 13-cis configuration.

Acknowledgments

We thank Dr. A. Weller for encouragement and support and Dr. Klaus Schulten for many discussions and for help with the manuscript. We are indebted to Dr. Jutta Peters for careful preparation of the samples. The large amount of purple membrane suspension needed for flow experiments was a gift from the laboratory of Dr. Oesterhelt, which is gratefully acknowledged.

References

Aton, B., Doukas, A. G., Callender, R. H., Becher, B., & Ebrey, T. G. (1977) *Biochemistry 16*, 2995.

Becher, B., & Ebrey, T. G. (1977) *Biophys. J. 17*, 182.

Becher, B., Tokunage, F., & Ebrey, T. G. (1978) *Biochemistry 17*, 2293.

Callender, R. H., & Honig, B. (1977) *Annu. Rev. Biophys. Bioeng. 6*, 33.

Callender, R. H., Doukas, A., Crouch, R., & Nakanishi, K. (1976) *Biochemistry 15*, 1621.

Campion, A., El-Sayed, M. A., & Terner, J. (1977) *Biophys. J. 20*, 369.

Cookingham, R., & Lewis, A. (1978) *J. Mol. Biol. 119*, 569.

Cookingham, R. E., Lewis, A., & Lemley, A. T. (1978) *Biochemistry 17*, 4699.

Dencher, N., & Wilms, M. (1975) *Biophys. Struct. Mech. 1*, 259.

Dencher, N. A., Rafferty, C. N., & Sperling, W. (1976) *Ber. Kernforschungsanlage Juelich 1364*, 1–42.

Dewar, M. J. S., & Ford, G. P. (1977) *J. Am. Chem. Soc. 99*, 1685.

Gill, D., Heyde, M. E., & Rimai, L. (1971) *J. Am. Chem. Soc. 93*, 6288.

Goldschmidt, C. R., Kalisky, O., Rosenfeld, T., & Ottolenghi, M. (1977) *Biophys. J. 17*, 179.

Henderson, R. (1977) *Annu. Rev. Biophys. Bioeng. 6*, 87.

Hess, B., & Kuschnitz, D. (1977) *FEBS Lett. 74*, 20.

Heyde, M. E., Gill, D., Kilponen, R. G., & Rimai, L. (1971) *J. Am. Chem. Soc. 93*, 6776.

Honig, B., Greenberg, A. D., Dinur, U., & Ebrey, T. G. (1976) *Biochemistry 15*, 4593.

Hurley, J. B., Becher, B., & Ebrey, T. G. (1978) *Nature (London) 272*, 87.

Inagaki, F., Tasumi, M., & Miyazawa, M. (1975) *J. Raman Spectrosc. 3*, 335.

Kalisky, O., Goldschmidt, C. R., & Ottolenghi, M. (1977) *Biophys. J. 19*, 185.

Kiefer, W., & Bernstein, H. J. (1971) *Appl. Spectrosc. 25*, 500.

Lewis, A., Spoonhower, J., Bogomolni, A., Lozier, R. H., & Stoeckenius, W. (1974) *Proc. Natl. Acad. Sci. U.S.A. 71*, 4462.

Lozier, R. H., & Niederberger, W. (1977) *Fed. Prod., Fed. Am. Soc. Exp. Biol. 36*, 1828.

Marcus, M. A., & Lewis, A. (1977) *Science 195*, 1330.

Marcus, M. A., & Lewis, A. (1978) *Biochemistry 17*, 4722.

Margulies, L., & Stockburger, M. (1979) *J. Raman Spectrosc. 8*, 26.

Mathies, R., Oseroff, A. R., & Stryer, L. (1976) *Proc. Natl. Acad. Sci. U.S.A. 73*, 1.

Mathies, R., Freedman, T. B., & Stryer, L. (1977) *J. Mol. Biol. 109*, 367.

Oesterhelt, D. (1976) *Angew. Chem. 88*, 16.

Oesterhelt, D., & Hess, B. (1973) *Eur. J. Biochem. 37*, 316.

Oesterhelt, D., & Stoeckenius, W. (1973) *Proc. Natl. Acad. Sci. U.S.A. 70*, 2853.

Oesterhelt, D., & Stoeckenius, W. (1974) *Methods Enzymol. 31*, 667.

Oesterhelt, D., Meentzen, M., & Schuhmann, L. (1973) *Eur. J. Biochem. 40*, 453.

Orlandi, G., & Schulten, K. (1979) *Chem. Phys. Lett. 64*, 370.

Oseroff, A. R., & Callender, R. H. (1974) *Biochemistry 13*, 4243.

Pettei, M. J., Yudd, A. P., Nakanishi, K., Henselmann, R., & Stoeckenius, W. (1977) *Biochemistry 16*, 1955.

Rimai, L., Gill, D., & Parsons, J. L. (1971) *J. Am. Chem. Soc. 93*, 1353.

Schulten, K. (1978) in *Energetics and Structure of Halophilic Microorganisms* (Caplan, S. R., & Ginzburg, M., Eds.) pp 331–334, Elsevier/North-Holland Biomedical Press, Amsterdam.

Schulten, K., & Tavan, P. (1978) *Nature (London) 272*, 85.

Sperling, W., Carl, P., Rafferty, D. N., & Dencher, N. A. (1977) *Biophys. Struct. Mech. 3*, 79.

Sperling, W., Rafferty, D. N., Kohl, K. D., & Dencher, N. A. (1979) *FEBS Lett. 97*, 129.

Stockenius, W. (1976) *Sci. Am. 234*, 38.

Terner, J., Hsieh, C. L., & El-Sayed, M. A. (1979) *Biophys. J. 26*, 527.

v. Grundherr, C., & Stockburger, M. (1973) *Chem. Phys. Lett. 22*, 253.

Warshel, A., & Karplus, M. (1974) *J. Am. Chem. Soc. 96*, 5677.

Warshel, A., & Dauber, P. (1977) *J. Chem. Phys. 66*, 5477.

Yariv, A., Ed. (1975) in *Quantum Electronics*, 2nd ed., pp 110–117, Wiley, New York.